Linkage Isomerization in Pt^{II}–9-Methyladenine Complexes

Jorma Arpalahti,*[a] Karel D. Klika,[a] and Satu Molander[a]

Keywords: Linkage isomerization / NMR spectroscopy / Nucleobases / Platinum / Structure elucidation

Bis(9-methyladenine) complexes of *cis*-$Pt^{II}(NH_3)_2$ undergo slow linkage isomerization from the N7 to the N1 site in aqueous solution at elevated temperatures. The ratio of the isomeric complexes during the isomerization process indicates that whilst Pt^{II} prefers the N(7) site in the adenine moiety kinetically, it is the N(1) coordination mode which is thermodynamically more stable. The crystal structures of the isomers do not reveal any unusual features; the few apparently structurally significant differences in the bond angles in the N(1)-bound bis(complex) merely reflect the poor quality of the crystal and/or crystal packing effects rather than a direct result emanating from the coordination mode of the ligand.

Introduction

Of the naturally occurring nucleobases, the adenine moiety exhibits the most flexible binding-site behavior with metal ions. In 9-substituted adenine derivatives, the ring nitrogens N(1) and N(7) are the predominant binding sites;[1] in aqueous solution the distribution of the metal ion between these sites depends on the pH, the metal, and the other ligands coordinated to the metal.[2] When coordination to both of these sites is blocked binding may then occur at N(3).[3] In exceptional cases, various metal ions may also bind to the exocyclic amino group with a concomitant loss of a proton.[4–6]

The site distribution of the metal ion is pH-dependent due to the different basicities of the adenine nitrogen atoms and in this respect, the N(1),N(7) dichotomy of 9-substituted adenines has received considerable attention. Whilst hard 3d transition metal ions slightly favor the N(7) site over the N(1) site,[7] softer metal species such as Pd^{II} appear to prefer the N(1) site.[1a] With inert cations like Pt^{II}, however, care must be taken to distinguish the kinetically preferred binding site from the thermodynamically more stable one. Recently, we have shown that monofunctional, aquated Pt^{II}(dien) kinetically favors the N(7) site in adenosine, although it is the N(1) binding mode which is thermodynamically more stable.[8] (The slow isomerization process takes several days at 65 °C in aqueous solution.) With bifunctional Pt^{II} compounds, such as the biologically important Pt^{II} diamines, the majority of studies reveal only N(7) coordination,[2,9] with only rare instances of the Pt^{II} binding to other sites in the adenine moiety such as N(1),[10–12] or N(6)[6b]. Although the Pt^{II}–N bond is generally considered inert, the relatively easy bond rearrangement found in platinated oligonucleotides[11b,13] have led to this dogma being questioned.[12] Together with the novel S→N migration of coordinated Pt in sulfur containing biomolecules,[14] this has led to tremendous interest in the linkage isomerization in Pt-nucleobase complexes.[6,12] In this work we report the isomerization of bis(9-methyladenine) complexes of *cis*-$Pt^{II}(NH_3)_2$ in aqueous solution. The isomeric complexes exhibiting the N(1),N(1); N(1),N(7); and N(7),N(7) binding modes of Pt^{II} in the adenine moiety have been structurally characterized by X-ray crystallography and by ^{1}H-, ^{13}C-, and ^{195}Pt-NMR spectroscopy. To our knowledge, the former two complexes represent the first examples of mononuclear Pt^{II} bis(complexes) in which the adenine moiety displays the N(1) binding mode.

Results and Discussion

The isomerization of the bis(complexes) of 9-methyladenine (9-made), *cis*-$[Pt(NH_3)_2$(9-made-*N*7)$_2]^{2+}$ (**1**), *cis*-$[Pt(NH_3)_2$(9-made–*N*1)(9-made-*N*7)$]^{2+}$ (**2**) *cis*-$[Pt(NH_3)_2$(9-made-*N*1)$_2]^{2+}$ (**3**), can be conveniently followed by HPLC (see Figure 1).

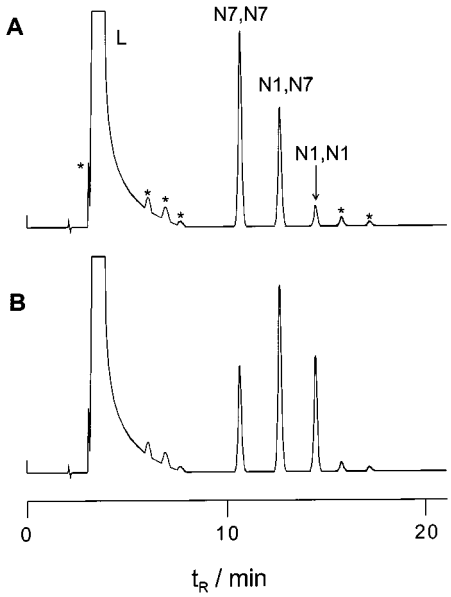

Figure 1. HPLC profiles of the isomerization mixture after 1 h (A) and 15 d (B). Notation: L is free 9-methyladenine, while the isomeric complexes are denoted as Pt binding sites; * denote unknown species

[a] Department of Chemistry, University of Turku,
FIN-20014, Turku, Finland
Fax: (internat.) + 358-2-333 6700
E-mail: jorma.arpalahti@utu.fi

  1434−1948/00/0505−1007 $ 17.50+.50/0

When compared to free nucleobase, the bis(complexes) have longer retention times and the complexes follow an elution order of **1** < **2** < **3**. In a solution containing a slight excess of the ligand ($[Pt]_T/[L]_T$ = 1:2.5), the N(7) coordination mode predominates at the beginning of complexation

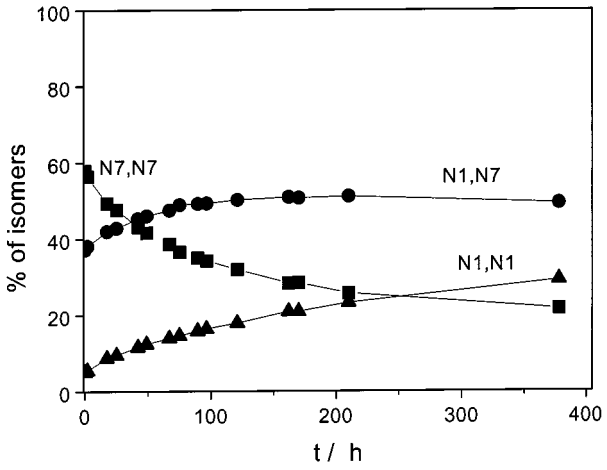

Figure 2. The relative percentage of different complexes (based on peak areas at 260 nm) during the isomerization process in aqueous solution at 80–85 °C

(Figure 2). However, when kept at ca. 85 °C for several days a slow N(7)→N(1) isomerization takes place, as shown by the diminution of the N(7),N(7)-bound species and an increase in the N(1),N(7)- and the N(1),N(1)-bound species. The time-dependent concentrations of the different complexes indicate that it is the N(7) binding mode which is kinetically preferred, whereas it is the N(1) site which forms the thermodynamically more stable complexes; this is in line with findings for monofunctional Pt^{II}.[8] Interestingly, the amount of the bis(complex) with the mixed N(1),N(7) coordination mode first increases and then only very slowly decreases indicating stepwise N(7)→N(1) isomerization. The slowness of the reaction, as compared to intramolecular bond rearrangements,[6] suggests that in this case the isomerization results from the breaking and reformation of Pt-nucleobase bonds. Unfortunately, the data do not allow definitive conclusion about the reaction path, i.e. solvent path and/or direct nucleophilic attack of the free nucleobase on the complex for both are expected to be very slow.[1b]

The kinetic preference of Pt^{II} for the adenine N(7) site may be attributed to steric hindrance by the exocyclic amino group that limits the platination of the N(1) site[7,10] despite its stronger basicity.[15] Because the N(7)→N(1) isomerization is slow even at elevated temperatures, reflecting the high thermodynamic stability of the Pt–N bond,[15] it is not surprising therefore that the formation of bis(complexes) exhibiting only the N(1) binding mode has been previously overlooked.[11a]

The ^1H, ^{13}C, and ^{195}Pt spectral data for the dications **1**, **2**, and **3** are listed in Table 1. All three complexes in aqueous solutions show evidence of dynamic processes, as indicated by the splitting and/or broadening of the ^1H, ^{13}C, and ^{195}Pt signals. In all likelihood, the dynamic process in effect is the restricted rotation of the nucleobase(s) about the Pt–N bond resulting from the close spatial proximity of the Pt^{II} atom and the exocyclic amino group of the adenine moiety. This spatial proximity is particularly close for the N(1)-bound species[6a,8] and consistent with this, **3** displays the strongest effects. Nevertheless, the observed ^1H chemical shifts corroborate the assignment of the Pt binding modes showing significant downfield shifts by those signals near the proposed coordination site. The δ_{Pt} values of all three isomeric complexes are close to –2500 ppm, typical for a PtN_4 coordination sphere.[16]

Crystal Stuctures

The crystal structure analyses confirmed the Pt^{II} binding modes of the isomeric complexes and the thermal ellipsoids of the dications of **1a – 3a** are shown in Figures 3, 4, and 5, respectively; selected interatomic distances and angles are listed in Table 2.

The crystallographic data, experimental details and results of structure refinements are listed in Table 3. In all complexes, the Pt^{II} coordination sphere is nearly square-planar with normal and very similar Pt–N bond lengths and angles, except in **1**, where the Pt–N(7a) distance of 2.021(6) Å seems to be significantly shorter (3.8σ[17]) than the Pt–N(11) distance of 2.056(7) Å. Otherwise the cation of **1a** is very similar to the corresponding one of the nitrate salt.[9] The complexed nucleobases are orientated in a head-to-tail fashion in **1** and **2**, whereas in **3** their orientation is head-to-head. The latter is of particular interest, as it brings the exocyclic C(6)–NH_2 groups onto the same side of the PtN_4 plane. The N(6)···Pt distance of 3.21(1) Å in **3** is close to that found in **2** for the N(1)-bound 9-made, viz. 3.149(8) Å, and comparable to those reported earlier for other N(1) platinated adenine derivatives.[6a,8] With the N(1) binding mode, the exocyclic amino group is significantly closer to the Pt^{II} atom than it is in N(7)-bound species; the N(6)···Pt distance is 3.446(8) Å in the N(7)-bound 9-made of **2,** and 3.430(7) Å (unit A) and 3.515(7) Å (unit B) in **1**. The close proximity of the Pt^{II} and N(6) atoms may indicate a hydrogen bond type of interaction between these two atoms. The calculated values for the N(6)H···Pt distances and the N(6)–H(6)···Pt angles of 2.76 Å and 114° [H(6B)] in **3**, 2.67 Å and 116° [H(6A1)], and 2.75 Å and 139° [H(6B2)] in **2**, 2.73 Å and 139° [H(6A2)], and 2.82 Å and 139° [H(6B2)] in **1** are, at least for the N(7)-bound species, close to the values given in the literature for this type of interaction, viz. 2.2–3.5 Å and >120°, respectively.[18] Irrespective of this interaction being present, the Pt^{II} atom lies virtually in the plane defined by the four coordinating nitrogen atoms and deviates by less than 0.02 Å from this plane in all three complexes.

The corresponding bond lengths and angles of the base moieties in **1** and **2** are very similar and they do not significantly deviate from the values given for uncomplexed 9-methyladenine.[19] The same holds true also for the bond lengths in **3**, where the several seemingly large differences become insignificant when the large e.s.d.s are taken into account, e.g. the C(4)–C(5) bond. However, some of the ring angles in **3** display significant changes when compared

Table 1. ^{1}H, ^{13}C, and ^{195}Pt chemical shifts in ppm for **1**, **2**, and **3**

Chem. shifts[a]		δ_{Pt}	δ_H			δ_C					
Compounds			H2	H8	CH_3	C2	C4	C5	C6	C8	CH_3
1[b]		–2476	8.292 {8.33} (8.240)[c]	8.628 {8.63} (8.764)[c]	3.799 {3.81}	156.41	151.75	118.23	156.45	147.03	33.56
2[d]	N(1)[e]	–2527	8.639 (8.826)	8.010 (8.040)	3.702 (3.759)	155.59 (155.25)	150.36 [f]	121.42 (121.31)[c]	157.90 (157.84)	147.30 [g]	32.63 [g]
	N(7)[e]		8.260 (8.224)	8.695 (8.844)	3.819 (3.836)	156.33 [g]	151.71 [f]	118.20 (118.34)[c]	156.37 [g]	147.16 (146.81)	33.57 [g]
3[h]		–2565 (–2583)	8.797 (8.883)	8.153 (8.158)	3.812 (3.829)	156.31 (155.28)	150.39 (150.46)	121.2 (121.0)	157.79[i] (157.96) [i]	147.09 (147.18)	32.82 (32.86)

[a] Spectra recorded in D_2O (^{1}H) or in H_2O/D_2O (^{13}C and ^{195}Pt). – [b] Possibly two sets of signals in a ratio of 9:1, the values for the minor species in parenthesis; data from ref. [9] in braces – [c] Questionable. – [d] Two sets of signals for each nucleobase in a ratio of ca. 8:2, data for the minor species in parenthesis. – [e] Binding mode of 9-made and associated ^{1}H and ^{13}C chemical shifts. – [f] Not observed. – [g] Known to be hidden beneath other signals from the 2-D spectra. – [h] Two signals in a ratio of ca. 2:1 were detected for all nuclei. The values in parenthesis refer to the minor signal. – [i] Signal shows a shoulder 0.06 ppm upfield.

Table 2. Selected interatomic distances and angles for isomeric complexes **1**, **2**, and **3**

	1		**2**		**3**
Pt–N(10)	2.037(7)		2.044(7)		2.046(8)
Pt–N(11)	2.056(7)		2.033(8)		
Pt–N(1)			2.046(7)		2.038(11)
Pt–N(7)	2.031(7)[a]	2.021(6)[b]	2.022(7)		
N(1)–C(2)	1.334(12)	1.330(12)	1.389(11)[c]	1.330(13)[d]	1.29(3)
N(1)–C(6)	1.365(12)	1.343(11)	1.366(11)	1.358(11)	1.42(3)
N(3)–C(2)	1.340(12)	1.338(12)	1.306(12)	1.315(13)	1.40(3)
N(3)–C(4)	1.355(11)	1.347(11)	1.348(11)	1.351(11)	1.45(5)
N(6)–C(6)	1.331(11)	1.326(10)	1.324(11)	1.338(12)	1.28(2)
N(7)–C(5)	1.405(10)	1.389(10)	1.394(11)	1.412(11)	1.41(3)
N(7)–C(8)	1.314(10)	1.320(10)	1.323(12)	1.316(12)	1.33(2)
N(9)–C(4)	1.375(11)	1.370(11)	1.368(11)	1.372(12)	1.40(2)
N(9)–C(8)	1.358(11)	1.350(11)	1.365(12)	1.357(11)	1.42(4)
N(9)–C(9)	1.460(10)	1.474(10)	1.456(11)	1.465(13)	1.44(3)
C(4)–C(5)	1.375(11)	1.377(11)	1.380(12)	1.379(12)	1.24(6)
C(5)–C(6)	1.394(11)	1.429(11)	1.394(12)	1.377(13)	1.34(4)
N(10)–Pt–N(11)	89.1(3)		89.8(3)		
N(7)–Pt–N(7)	90.9(3)				
N(1)–Pt–N(7)			90.7(3)		
N(1)–Pt–N(1)#[e]					88.9(5)
N(1)–Pt–N(10)			179.2(3)		179.1(15)
N(1)–Pt–N(10)#[f]					90.7(4)
N(1)–Pt–N(11)			90.8(3)		
N(7)–Pt–N(10)	177.7(3)[a]	90.9(3)[b]	88.7(3)		
N(7)–Pt–N(11)	89.2(3)	179.7(3)	178.1(3)		
C(2)–N(1)–C(6)	119.0(8)	119.8(8)	119.0(7)[c]	118.3(9)[d]	119.6(11)
C(2)–N(3)–C(4)	110.4(7)	110.6(7)	112.1(8)	110.6(8)	107(2)
C(5)–N(7)–C(8)	106.4(7)	105.5(7)	103.5(8)	106.6(8)	109(2)
C(4)–N(9)–C(8)	106.0(6)	107.1(7)	106.4(7)	106.5(8)	91(3)
C(4)–N(9)–C(9)	126.9(8)	127.0(8)	127.9(8)	127.6(8)	143(3)
C(8)–N(9)–C(9)	127.0(8)	126.0(8)	125.3(8)	125.7(8)	125.4(17)
N(1)–C(2)–N(3)	129.3(9)	128.8(9)	127.7(8)	129.9(9)	127(2)
C(5)–C(4)–N(9)	108.1(7)	106.5(7)	106.0(8)	108.3(8)	127(4)
C(5)–C(4)–N(3)	126.0(8)	127.3(7)	125.9(8)	125.4(9)	130.2(17)
N(3)–C(4)–N(9)	125.9(7)	126.2(7)	128.1(8)	126.3(8)	103(4)
C(4)–C(5)–C(6)	118.8(8)	116.4(7)	119.3(8)	118.6(8)	119(3)
C(4)–C(5)–N(7)	107.2(7)	108.9(7)	110.6(8)	106.7(8)	98(3)
C(6)–C(5)–N(7)	133.9(7)	134.7(7)	130.1(8)	134.7(9)	142(4)
C(5)–C(6)–N(6)	125.3(8)	124.5(8)	123.5(8)	124.8(8)	117(3)
C(5)–C(6)–N(1)	116.5(8)	117.1(7)	115.9(8)	117.1(9)	118(3)
N(1)–C(6)–N(6)	118.2(8)	118.4(8)	120.6(8)	118.1(8)	125(2)
N(7)–C(8)–N(9)	112.2(7)	112.1(7)	113.5(8)	111.9(8)	114.1(14)

[a] Unit A. – [b] Unit B. – [c] For N(1)-bound 9-made (unit A). – [d] For N(7)-bound 9-made (unit B). – [e] N(1)# generated by symmetry transformation: $-x + 3/2, y, z$. – [f] N(10)# generated by symmetry transformation: $-x+3/2, y, z$.

Table 3. Crystal data and structure refinement for the isomeric complexes *cis*-$[Pt(NH_3)_2(9\text{-made-}N7)_2](ClO_4)_2 \cdot 2\,H_2O$ (**1a**), *cis*-$[Pt(NH_3)_2(9\text{-made-}N1)(9\text{-made-}N7)](ClO_4)_2$ (**2a**), and *cis*-$[Pt(NH_3)_2(9\text{-made-}N1)_2](PF_6)_2 \cdot 3\,H_2O$ (**3a**)

	1	**2**	**3**
Empirical formula	$C_{12}H_{24}Cl_2N_{12}O_{10}Pt$	$C_{12}H_{20}Cl_2N_{12}O_8Pt$	$C_{12}H_{26}F_{12}N_{12}O_3P_2Pt$
Molecular mass	762.42	726.39	871.48
Crystal system	triclinic	triclinic	orthorhombic
Spące group	*P*–1	*P*–1	*Ama*2
a [Å]	9.564(3)	10.2393(10)	20.875(3)
b [Å]	16.117(5)	15.455(3)	15.524(4)
c [Å]	7.9983(14)	7.4399(10)	8.742(6)
α [°]	91.995(19)	98.614(12)	90
β [°]	90.69(3)	91.663(9)	90
χ [°]	104.68(3)	89.441(10)	90
V [Å^3]	1191.7(6)	1163.6(3)	2833(2)
Z	2	2	4
D(calcd.) [g cm^{-3}]	2.125	2.073	2.043
μ [mm^{-1}]	6.188	6.326	5.185
F(000)	744	704	1688
Crystal size [mm]	0.12 × 0.34 × 0.36	0.12 × 0.14 × 0.18	0.20 × 0.20 × 0.16
θ range [°]	1.31–25.05	1.99–25.16	1.95–27.49
Index ranges	+11, ±19, ±10	+12, ±18, ±9	+27, –20, +11
Reflections collected	4206	4343	1785
independent (R_{int})	4206 (0.0000)	4096 (0.0364)	1785 (0.0000)
observed [$I > 2\sigma I$]	3665	3359	1170
Absorption correction	ψ scan		
Transmission	1.000–0.661	1.000–0.667	1.000–0.696
Refinement method	Full-matrix least-squares on F^2		
Data/restraints/parameters	4026/10/334	4096/42/311	1785/13/199
Goodness-of-fit on F^2	1.065	1.078	1.038
R indices[a] [$I > 2\sigma I$]	$R_1 = 0.0401$	$R_1 = 0.0387$	$R_1 = 0.0422$
	$wR2 = 0.0991$	$wR2 = 0.0890$	$wR2 = 0.0785$
R indices (all data)	$R_1 = 0.0532$	$R_1 = 0.0654$	$R_1 = 0.1021$
	$wR2 = 0.1047$	$wR2 = 0.1004$	$wR2 = 0.0926$
Largest diff. peak and hole [eÅ^{-3}]	2.125 and –2.240	1.569 and –1.247	1.372 and –0.926

[a] $R_1 = \Sigma||F_o| - |F_c||/\Sigma|F_o|$, $wR_2 = \{\Sigma\,[w(F_o^2 - F_c^2)^2]/\Sigma\,[\,w(F_o^2)^2]\}^{1/2}$ and $w = 1/[\sigma^2(F_o^2) + (aP)^2 + bP)]$, where $P = (2\,F_c^2 + F_o^2)/3$.

to isomers **1** and **2** and to the uncomplexed ligand. The most significant difference can be seen in the N(3)–C(4)–N(9) angle of 103(4)°, which differs by 6.2σ[17] from that in the N(1)-bound 9-made of **2**, viz.128.1(8)°. Other significant differences include the angles C(4)–N(9)–C(8) (5.2σ from that in **1**, unit B), C(4)–N(9)–C(9) (5.2σ from that in **1**, unit A), C(5)–C(4)–N(9) (5.1σ) and C(4)–C(5)–N(7) (4.1σ) from that in **2** [N(1)-bound 9-made]. It seems to us that these differences merely reflect the poor quality of the crystal and/or crystal packing effects rather than a direct result emanating from the coordination mode of the ligand,[20] since the majority of the significant differences are seen relative to the N(1)-bound ligand in **2**.

The packing of the isomeric complexes is predominantly stabilized by hydrogen bonding involving primarily the am(m)ine hydrogens and anions and/or lattice water (Table 4). Additional H-bonds may be formed between the exocyclic amino groups and endocyclic nitrogens in **2a**, and between water molecules in **1a** and **3a**. By contrast, stacking of the base moieties seems to be relative unimportant in stabilizing the crystal lattice. In **1a**, the neighboring bases are orientated in a head-to-tail fashion with a distance of 3.64 Å between the centers of the 5- and 6-membered rings, which may indicate a weak stacking interaction. With **2a** and **3a**, the distances between the neighboring heteroaromatic rings are > 4 Å.

Conclusions

The isomerization of the bis(9-methyladenine) complexes of *cis*-$Pt^{II}(NH_3)_2$ in aqueous solution is a very slow process. The ratio of the isomeric complexes as a function of time indicates that Pt^{II} kinetically prefers the N(7) site in the adenine moiety, whilst it is the N(1) coordination mode which is thermodynamically more stable. The slowness of the reaction, as compared to the intramolecular Pt^{II}–N bond rearrangement,[6b] suggests that the isomerization of the bis(complexes) results from the breaking and reformation of Pt-nucleobase bonds, although no definitive conclusion about the reaction path can be made. In this respect, the relative easy bond rearrangements in platinated oligonucleotides (single stranded or double stranded)[11b,13] are strongly suggestive for an intramolecular migration mechanism. The crystal structures of the isomers do not reveal any unusual features, except for those few apparently significant differences in the bond angles in the N(1)-bound bis(complex), which merely reflect the poor quality of the crystal and/or crystal packing effects rather than a direct result emanating from the coordination mode of the ligand. The packing of the isomeric complexes is predominantly stabilized by hydrogen bonding, whilst stacking of the base moieties seems to be relative unimportant in stabilizing the crystal lattice.

Table 4. Possible hydrogen bonds (D–H···A) for **1a – 3a**

D–H···A[a]	*d*(D···A) [Å]; <(DHA) [°]	Symmetry transformation
Compound **1a**		
N(6A)–H(6A1)···N(1A)	3.05(1); 156.4	$-x, -y + 1, -z + 2$
N(6B)–H(6B1)···N(1B)	3.02(1); 171.1	$-x + 1, -y, -z + 2$
N(10)–H(10A)···O(6)	3.00(1); 168.5	$x - 1, y, z$
N(10)–H(10C)···O(1)	3.09(1); 163.6	
N(11)–H(11C)···N(3A)	3.01(1); 170.1	$-x + 1, -y + 1, -z + 2$
N(11)–H(11A)···O(7)	3.02(1); 167.3	$x - 1, y, z$
N(11)–H(11B)···O(2)	3.05(1); 167.0	
O(9)···O(10)	2.80(1)	$x, y, z - 1$
O(9)···O(3)	2.98(2)	
O(9)···O(8)	2.86(2)	
O(10)···O(5)	2.71(3)	
Compound **2a**		
N(6A)–H(6A1)···O(2A)	2.78(2); 135.8	$x, y, z + 1$
N(6A)–H(6A2)···N(7A)	2.94(1): 157.8	$-x + 1, -y + 2, -z + 2$
N(6B)–H(6B1)···N(1B)	3.00(1); 168.2	$-x + 2, -y + 1, -z + 1$
N(10)–H(12B)···O(6A)	2.73(2); 131.6	
N(10)–H(12C)···O(4A)	3.02(2); 152.8	$x, y, z + 1$
N(11)–H(11B)···O(7A)	2.94(2); 165.7	$-x + 1, -y + 1, -z + 2$
N(11)–H(11A)···O(6B)	3.03(2); 163.6	
Compound **3a**		
N(6)–H(6A)···O(1A)	2.78(7); 166.8	
N(6)–H(6B)···F(2)	2.83(5); 128.7	$x, y + {}^1/_2, z + {}^1/_2$
N(10)–H(10B)···O(2B)	2.94(7); 144.7	$x, y + {}^1/_2, z - {}^1/_2$
N(10)–H(10B)···O(2A)	2.96(3); 166.7	$x, y + {}^1/_2, z - {}^1/_2$
O(1B)···O(2A)	2.55(3)	
O(1B)···O(2B)	2.86(9)	

[a] The water hydrogens could not be located from the electron density maps.

Experimental Section

General Remarks: The NMR measurements were carried out in D_2O (^1H) or in H_2O/D_2O (^{13}C and ^{195}Pt) at ambient temperature. Spectra were acquired on a JEOL Alpha 500 spectrometer equipped with a 5 mm tunable probe operating at 500.16 MHz for ^1H, 125.78 MHz for ^{13}C, and 107.21 MHz for ^{195}Pt.[8] The ^1H and ^{13}C spectra were referenced internally to sodium 4,4-dimethyl-4-silapentanesulfonate (DSS), assigned as $\delta = 0.015$ ppm for proton and 0 ppm for carbon; the ^{195}Pt spectra were referenced externally to $[PtCl_4]^{2-}$ (δ_{Pt} –1625 ppm from $[PtCl_6]^{2-}$). The assignments of the ^1H and ^{13}C resonances were based on HMQC, DEPT, and HMBC spectra and by comparison to the assignments of the Pt^{II}(dien) complexes of adenosine.[8] – The HPLC measurements were carried out on a Merck-Hitachi chromatograph using an end-capped RP-18 column (5 μm, E. Merck AG) and a water/methanol (85:15) mixture (0.05 M $NaClO_4$, pH 3) as eluent. – Adenine was purchased from Sigma, $NaClO_4 \cdot H_2O$ and DMF from E. Merck AG, and $NaPF_6$ (98%) from Ventron; all were used as received.

Isomerization Procedure: Treatment of *cis*-$[PtI_2(NH_3)_2]$[21] (970 mg, 2.0 mmol) with two equivalents of $AgNO_3$ in 10 mL of water for two hours at 60 °C gave a clear solution of the diaqua species upon removing the AgI precipitate by filtration. After the addition of 9-methyladenine[22] (9-made, 550 mg, 3.7 mmol) into 7.4 mL of the Pt^{II} solution, the mixture was stirred at 80–85 °C and the progress of the isomerization was intermittantly followed by HPLC. After 15 days, the reaction was stopped (the mixture began to turn yellow together with the formation of some black solid), the mixture was filtered, and the filtrate was left to evaporate to dryness at ambient temperature. The solid residue was treated with 30 mL of boiling methanol to remove most of the unchanged 9-made. According to HPLC analysis the remaining solid residue (620 mg) contained ca. 20% of 9-made and ca. 75% of the desired isomers. The isomeric complexes were isolated and purified by fractional crystallization with different anions, as described below.

***cis*-[Pt(NH$_3$)$_2$(9-made-*N*7)$_2$](ClO$_4$)$_2$ · 2 H$_2$O (1a):** The crude product obtained above was dissolved in 2 mL of water with gentle warming. Slow cooling to +4 °C afforded a crystalline product with a composition of [**2**] ≈ [**1**] > [**3**] as deduced by HPLC analysis. Repeated recrystallizations from a minimal amount of water finally gave ca. 50 mg of chromatographically pure crystals of **1** with NO_3^- as the counter ion. Alternatively, and more conveniently, **1** was prepared by dissolving 9-made (120 mg, 0.8 mmol) in 2 mL of 1 M HNO_3 [to prevent N(1) platination], followed by the addition of 0.38 equiv. of *cis*-$[Pt(NH_3)_2(H_2O)_2]^{2+}$ in 5 mL of water. After stirring for 48 h at ca. 35 °C, the filtered solution was neutralized with 1 M NaOH, which afforded 125 mg of pale yellow crystals (50% from Pt) upon cooling to +4 °C. The isomeric purity of the product (>99%) was ascertained by HPLC analysis. Finally, **1** was crystallized as a perchlorate (**1a**) by dissolving the dinitrate in 1 M $NaClO_4$. – $C_{12}H_{24}Cl_2N_{12}O_{10}Pt$ (762.42): calcd. C 18.90, H 3.17, N 22.05; found C 18.80, H 3.02, N 21.82.

***cis*-[Pt(NH$_3$)$_2$(9-made-*N*1)(9-made-*N*7)](ClO$_4$)$_2$ (2a):** All of the solutions obtained from the above fractional crystallizations were pooled, which gave a mixture with a relative composition of [**2**] > [**3**] > [**1**]. This solution was concentrated to ca. 1 mL; after the addition of 1 mL of 1 M $NaClO_4$ to the mixture, crystals (ca. 320 mg) were obtained at +4 °C. The filtered crystalline product was then dissolved in 1.5 mL of DMF.[23] Crude **2a**, obtained at –20 °C after the addition of 0.2 mL of water and 6 mL of ethanol to the solution, was filtered off and washed with cold water. Recrystallization from a minimal amount water gave 120 mg of chromatographically pure **2a**. – $C_{12}H_{20}Cl_2N_{12}O_8Pt$ (726.39): calcd. C 19.84, H 2.78, N 23.14; found C 19.91, H 2.91, N 22.72.

***cis*-[Pt(NH$_3$)$_2$(9-made-*N*1)$_2$](PF$_6$)$_2$ · 3 H$_2$O (3a):** The DMF solution and washings of **2a** were evaporated to dryness at ambient temperature. The solid residue was washed with cold 0.1 M $HClO_4$ to remove most of the remaining **2a**. Dissolving the residue in 1 mL of water yielded 50 mg of chromatographically pure **3a** at +4 °C after the addition of 1 mL of 1 M $NaPF_6$ (pH 5, adjusted with 1 M NaOH) to the solution. – $C_{12}H_{26}F_{12}N_{12}O_3P_2Pt$ (871.48): calcd. C 16.54, H 3.01, N 19.29; found C 16.41, H 2.81, N 18.98.

X-ray Diffraction Studies: All X-ray data were collected on a Rigaku AFC5S diffractometer at ambient temperature with Mo-K_α radiation (λ = 0.71069 Å). Unit cell parameters were obtained from a least-squares fit of 25 reflections [41.60 < 2θ < 45.48° (**1a**), 40.82 < 2θ < 46.60° (**2a**), and 20.95 < 2θ < 31.61° (**3a**)]. Intensity data were collected by the ω/2θ scan technique to a maximum 2θ value of 50° (55° for **3a**). The intensities of three standard reflections were measured every 150 data points in all cases, and they showed no intensity decay. The intensities of the reflections were corrected for Lorenz, polarisation and absorption (empirical) effects.[24] The structures were solved by standard Patterson and difference Fourier methods and refined by full-matrix least-squares calculations employing SHELXL-97.[25] All atoms except hydrogen were refined with anisotropic temperature factors. In all complexes the hydrogen atoms are at the calculated positions. The final cycle of refinement gave for the structure **1a**, R_1 = 0.0401 and $wR2$ = 0.0991 for the observed data [$I > 2\sigma(I)$] and 334 parameters and R_1 = 0.0532 and $wR2$ = 0.1047 for all data. For **2a**, refinement converged at R_1 = 0.0387 and $wR2$ = 0.0890 for the observed data and 311 parameters and R_1 = 0.0654 and $wR2$ = 0.1004 for all data. For **3a** the final refinement cycle gave R_1 = 0.0422 and $wR2$ = 0.0785 for the observed data and 200 parameters and R_1 = 0.1021 and $wR2$ = 0.0926 for all data. Crystallographic data and experimental details are given in Table 2, selected bond lengths and angles are given in Table 3, and possible hydrogen bonds in Table 4. Data reduction and subsequent calculations were performed with *teXsan for Windows*.[26] Figures were drawn with *Ortep-3 for Windows*.[27] Crystallographic data (excluding structure factors) for the structures reported in this paper have been deposited with the Cambridge Crystallographic Data Centre as supplementary publication no. CCDC-135162 (**1a**), CCDC-135163 (**2a**), and CCDC-135164 (**3a**). Copies of the data can be obtained free of charge on application to CCDC, 12 Union Road Cambridge, CB2 1EZ, UK [Fax: +44 (0)1223/336-033; E-mail: deposit@ccdc.cam.ac.uk].

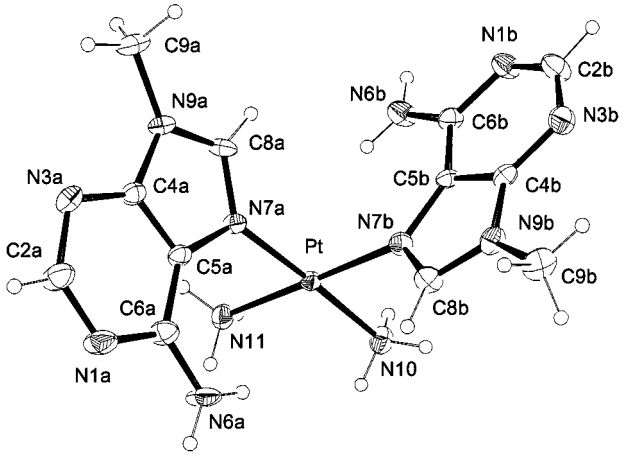

Figure 3. ORTEP plot of the cation of *cis*-[Pt(NH$_3$)$_2$(9-made-*N*7)$_2$](ClO$_4$)$_2$ · 2 H$_2$O (**1a**) showing 30% probability ellipsoids

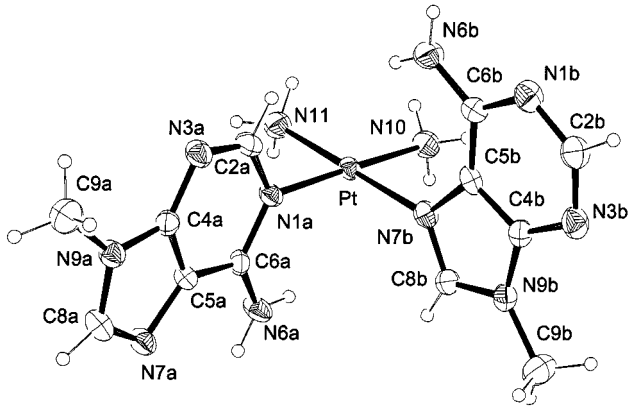

Figure 4. ORTEP plot of the cation of *cis*-[Pt(NH$_3$)$_2$(9-made-*N*1)(9-made-*N*7)](ClO$_4$)$_2$ (**2a**) showing 30% probability ellipsoids

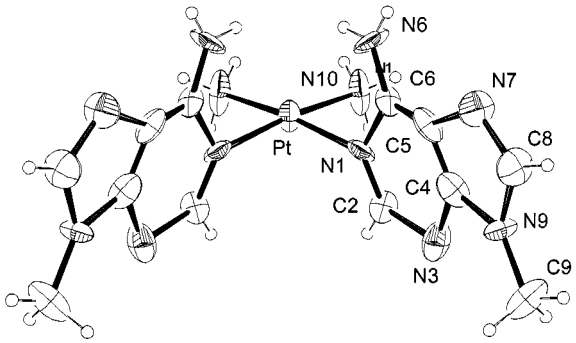

Figure 5. ORTEP plot of the cation of *cis*-[Pt(NH$_3$)$_2$(9-made-*N*1)$_2$](PF$_6$)$_2$ · 3 H$_2$O (**3a**) showing 30% probability ellipsoids

Acknowledgments

We thank Dr. Reijo Sillanpää for helpfull discussions concerning the X-ray crystal structure analysis. This work is a part of the COST Action D8/004/97 (Chemistry of Metals in Medicine).

[1] [1a] R. B. Martin, in: *Cisplatin – Chemistry and Biochemistry of a Leading Anticancer Drug* (Ed.: B. Lippert). Verlag Helvetica Chimica Acta, Zürich, **1999**, 183–205. – [1b] J. Arpalahti, in: *Cisplatin – Chemistry and Biochemistry of a Leading Anticancer Drug* (Ed.: B. Lippert). Verlag Helvetica Chimica Acta, Zürich, **1999**, 207–222.
[2] B. Lippert, in: *Progress in Inorganic Chemistry, Vol. 37* (Ed.: S. J. Lippard). Wiley, New York, **1989**, 1–97.
[3] C. Meiser, B. Song, E. Freisinger, M. Peilert, H. Sigel, B. Lippert, *Chem. Eur. J.* **1997**, *3*, 388–398.
[4] [4a] L. Y. Kuo, M. G. Kanatzidis, M. Sabat, A. L. Tipton, T. J. Marks, *J. Am. Chem. Soc.* **1991**, *113*, 9027–9045. – [4b] F. Zamora, M. Kunsman, M. Sabat, B. Lippert, *Inorg. Chem.* **1997**, *36*, 1583–1587.
[5] [5a] M. J. Clarke, *J. Am Chem. Soc.*, **1978**, *100*, 5068–5075. – [5b] G. Lowe, T. Vilaivan, *Perkin Trans. 1*, **1996**, 1499–1503.
[6] [6a] J. Arpalahti, K. D. Klika, *Eur. J. Inorg. Chem.* **1999**, 1199–1201. – [6b] J. Viljanen, K. D. Klika, R. Sillanpää, J. Arpalahti, *Inorg. Chem* **1999**, *38*, 4924–4925.
[7] J. Arpalahti, E. Ottoila, *Inorg. Chim. Acta* **1985**, *107*, 105–110.
[8] J. Arpalahti, K. D. Klika, R. Sillanpää, R. Kivekäs, *Dalton Trans.* **1998**, 1397–1402.
[9] A. Iakovidis, N. Hadjiliadis, F. Dahan, J.-P. Laussac, B. Lippert, *Inorg. Chim. Acta*, **1990**, *175*, 57–63.

[10] J. Arpalahti, P. Lehikoinen, *Inorg. Chim. Acta* **1989**, *159*, 115–120.
[11] [11a] A. Eastman, *Biochemistry* **1982**, *21*, 6732–6736. – [11b] K. Inagaki, M. Alink, A. Nagai, Y. Kidani, J. Reedijk, *Inorg. Chem*. **1990**, *29*, 2183–2185.
[12] B. Lippert, *Coord. Chem. Rev.* **1999**, *182*, 263–295.
[13] [13a] S. L. Bruhn, J. H. Toney, S. J. Lippard, in: *Progress in Inorganic Chemistry, Vol. 38* (Ed.: S. J. Lippard). Wiley, New York, **1990**, 477–516. – [13b] M. Boudvillain, R. Dalbiès, M. Leng, in: *Metal Ions in Biological Systems, Vol. 33* (Eds.: A. Sigel, H. Sigel). Marcel Dekker, New York, **1996**, 87–103. – [13c] D. Yang, S. S. G. E. van Boom, J. Reedijk, J. H. van Boom, A. H.-J. Wang, *Biochemistry*, **1995**, *34*, 12912–12920.
[14] J. Reedijk, J. M. Teuben, in: *Metal Ions in Biological Systems, Vol. 32* (Eds.: A. Sigel, H. Sigel). Marcel Dekker, New York, **1996**, 339–362.
[15] M. Mikola, K. D. Klika, A. Hakala, J. Arpalahti, *Inorg. Chem*. **1999**, *38*, 571–578.
[16] T. G. Appleton, J. R. Hall, S. F. Ralph, *Inorg. Chem*. **1985**, *24*, 4685–4693.
[17] σ defined as $\sigma = (\sigma_1^2+\sigma_2^2)^{1/2}$ with σ_1 and σ_2 being the errors in angles that are compared (see ref. [4b]).
[18] [18a] W. Yao, O. Eisenstein, R. H. Crabtree, *Inorg. Chim. Acta* **1997**, *254*, 105–111. – [18b] D. Braga, F. Grepioni, E. Tedesco, K. Biradha, G. R. Desiraju, *Organometallics* **1997**, *16*, 1846–1856.
[19] [19a] T. J. Kistenmacher, M. Rossi, *Acta Crystallogr*. **1977**, *B33*, 253–257. – [19b] R. K. McMullan, P. Benci, B. M. Craven, *Acta Crystallogr*. **1980**, *B36*, 1424–1430.
[20] The employment of NO_3^- or ClO_4^- as the counter ion gave crystals of very poor quality.
[21] S.C. Dhara, *Indian J. Chem*. **1970**, *8*, 194–194.
[22] H. Lönnberg, J. Ylikoski, J. Arpalahti, E. Ottoila, A. Vesala, *Acta Chem. Scand.* **1985**, *A39*, 171–180.
[23] According to HPLC analysis the crystalline product contained **2** (80%) and **3** (20%); this ratio could not be changed by repeated recrystallizations from water.
[24] A. C. T. North, D. C. Phillips, F. S. Mathews, *Acta Crystallogr*. **1968**, *A24* 351–359.
[25] G. M. Sheldrick, *SHELXL 97*, *Program for the Refinement of Crystal Structures*, University of Göttingen, **1997**.
[26] *teXsan for Windows. Structure Analysis Software,* Molecular Structure Corporation, Texas 77381, USA (1997).
[27] L. J. Farrugia, *J. App. Cryst.,* **1997**, *30*, 565.

Received October 4, 1999
[I99344]